Journal of Hazardous Materials 168 (2009) 430–437

Contents lists available at ScienceDirect

Journal of Hazardous Materials

journal homepage: www.elsevier.com/locate/jhazmat

Arsenic removal by iron-doped activated carbons prepared by ferric chloride forced hydrolysis

V. Fierro[a,*], G. Muñiz[a,b], G. Gonzalez-Sánchez[c], M.L. Ballinas[b], A. Celzard[a,d]

[a] Institut Jean Lamour-UMR CNRS 7198, CNRS-Nancy-Université-UPVM, Faculté des Sciences & Techniques, BP 239, 54506 Vandœuvre-lès Nancy, France
[b] Facultad de Ciencias Químicas, Universidad Autónoma de Chihuahua, Circuito Universitario S/N, Chihuahua, Mexico
[c] Centro de Investigación en Materiales Avanzados (CIMAV), Miguel de Cervantes 120 Compl. Ind. Chih. 31109, Chihuahua, Mexico
[d] Institut Jean Lamour-UMR CNRS 7198, CNRS-Nancy-Université-UPVM, ENSTIB, 27 rue du Merle Blanc, BP 1041, 88051 Epinal cedex 9, France

ARTICLE INFO

Article history:
Received 21 October 2008
Received in revised form 23 January 2009
Accepted 9 February 2009
Available online 20 February 2009

Keywords:
Activated carbon
Arsenic removal
Iron
Forced hydrolysis
Ground water

ABSTRACT

Ferric chloride forced hydrolysis is shown to be a good method for increasing the iron content of activated carbons (ACs). Iron content increased linearly with hydrolysis time, and ACs with iron content as high as 9.4 wt.% at 24 h hydrolysis time could be prepared. The increase in iron content did not produce any modification in the textural parameters determined by nitrogen adsorption at 77 K. Iron-based nanoparticles, homogeneous in size and well-dispersed in the carbon matrix, were obtained. Nanoparticles forming iron (hydr)oxide agglomerates at the outer surface of the carbon grains at hydrolysis times higher than 6 h were also produced.

The AC obtained after 6 h of ferric chloride forced hydrolysis removed 94% of the arsenic present in a groundwater from the State of Chihuahua (Mexico), whereas the commercial AC used as precursor allowed the removal of only 14%. The lower performance in arsenic removal observed for AC prepared using long forced hydrolysis time (24 h) is probably due to the existence of iron (hydr)oxides nanoparticles agglomerates, which once hydrated could prevent diffusion of arsenate ($HAsO_4^-$) towards the inner surface of the AC grain.

1. Introduction

The northern part of Mexico has been affected by arsenic pollution for many years. During the eighties, concentrations of arsenic as high as 600 $\mu g\,L^{-1}$ were reported in the waters of the States of Coahuila and Durango, and especially in the region called Comarca Lagunera. Furthermore, arsenic levels as high as 500 $\mu g\,L^{-1}$ [1] were measured in the State of Chihuahua, in the region of Delicias–Meoqui. The reduction by the Secretaria del Medio Ambiente, Recursos Naturales y Pesca (SEMARNAP) to 10 $\mu g\,L^{-1}$ of the maximum allowed arsenic level in drinking water forces non compliant water supply systems [2] to implement additional treatment processes to produce finished water with arsenic levels within regulatory standards.

So far, a variety of methods have been developed for arsenic removal from drinking water. The technology of adsorption is based on materials having a high affinity for dissolved arsenic. Adsorption of arsenic by iron compounds has been established by several authors [3–5]. Elementary iron [6–8], granular iron hydroxides and ferrihydrites [9–12] have been proposed for the removal of arsenic from water. Most of the adsorption processes investigated so far were reported in the excellent review of Mohan and Pittman [13], whereas the other techniques were considered in that of Choong et al. [14].

Activated carbons (ACs) are by far the most widely used adsorbents for water treatment, even if arsenic removal is mainly achieved by other kinds of adsorbents (like GFH and SORB33) or coagulation/(micro) filtration using ferric chloride. ACs have been tested by many authors for arsenic removal, but their corresponding adsorption capacities are not satisfactory in a variety of situations. They are indeed strongly dependent on the physico-chemical properties of the solution, and hence on arsenic speciation; for example, adsorption capacities are very low at high pH (typically higher than nine) [15,16].

Huang and Vane have found that impregnation with different iron salts increased ten times the original arsenic adsorption capacity of carbon [17,18]. Moreover, the ability of removing other pollutants from water, and the possibility to take advantage of existing fixed-bed systems, is an additional advantage of carbonaceous adsorbents [19]. Gu et al. [20] prepared and evaluated granular activated carbon adsorbing iron (II) in the presence of sodium hypochlorite; high iron loadings (7 wt.%) were obtained. With such ACs doped with iron, it was possible to remove more than 80% of the arsenic [20]. Iron (III) impregnation is also effective, increasing

* Corresponding author. Fax: +33 383684619.
E-mail address: Vanessa.Fierro@lcsm-uhp.nancy.fr (V. Fierro).

0304-3894/$ – see front matter © 2009 Published by Elsevier B.V.
doi:10.1016/j.jhazmat.2009.02.055

anionic adsorption in a wider range of pHs. It is reported that inner sphere complexes between iron and arsenic could be formed for $pH < pH_{ZC}$ [19,21].

Activated carbon impregnation using a solution of iron salt is the most frequent method for doping activated carbons. In a previous study [22], raw and oxidised ACs were also doped with iron through treatments with either ferric chloride ($FeCl_3$) or ferrous chloride ($FeCl_2$) solutions at different pHs and concentrations. The higher efficiency of the iron-doped materials prepared from low concentration (0.05 M) $FeCl_3$ and $FeCl_2$ solutions was associated to the higher dispersion of iron in the ACs. In that study [22], a clear relationship between iron content and arsenic adsorption was evidenced, at the condition that iron is well-dispersed.

The forced hydrolysis of inorganic iron (III) salts has been extensively studied by Matijević et al. [23–25] and a complete review of the reaction of hydrolysis and precipitation in aqueous Fe (III) solutions was carried out by Flynn [26]. Jang et al. [27] modified ACs by two methods: iron-impregnation/precipitation and iron impregnation/evaporation using $Fe(NO_3)_3{\cdot}9H_2O$. In the first case, carbon was impregnated with the iron solution at pH 2.0–3.2, and the pH was subsequently increased to 4–5 for precipitating iron. In the second case, the pH was not modified after impregnation, and the mixture was heated at 100 °C until dry. These authors found that iron deposited onto the outer surface peeled off during use, and that the iron efficiency for removing arsenic was not always proportional to their iron content.

The challenge of this study was to increase the iron content of the doped ACs, but simultaneously to maintain a good dispersion and availability of particles, in order to allow arsenate ($HAsO_4^-$) diffusion and increase arsenic adsorption. With this aim in view, an AC oxidized beforehand was impregnated for 2 h in a 0.05 M $FeCl_3$ solution (in 3 M HCl), and the latter was hydrolyzed at 100 °C for different times, namely 1, 3, 6 and 24 h. The resultant iron-doped ACs were characterized, and their performances for arsenic removal were tested, using groundwater samples with an arsenic concentration of 300 ppb from a well from the State of Chihuahua (Mexico). The improved efficiency for arsenic removal of the iron-doped activated carbons was determined taking as a reference the raw, commercial, AC.

2. Experimental

2.1. Materials

Part of the composition of the Mexican well water used in the present study is given in Table 1; the total arsenic concentration is close to 300 ppb. The amounts of total organic carbon, fluoride and silica, i.e., compounds known to compete with arsenic for adsorption sites, were not determined, but the same water batch was used for all the experiments; the rigorous comparison of adsorption performances of various carbonaceous adsorbents, aim of the present study, was thus possible. Redox and pH conditions control the speciation of arsenic, which mainly exists as arsenate (As (V)) and arsenite (As (III)) after dissolution. Arsenate is typically present in the monovalent $H_2AsO_4^-$ and divalent $HAsO_4^{2-}$ anionic forms in oxygenated waters, while arsenite principally occurs in the neutral form, $HAsO_2$, in waters of pH lower than 9.0. For typical pH of natural waters (pH 5–8), arsenate exists as an anion, while arsenite remains fully protonated and is thus present as a neutral species.

The removal of arsenic from water was carried out using modified activated carbons derived from the commercial material NC-100, supplied by the company PICA (Vierzon, France).

2.2. Oxidation of the activated carbon

NC-100 carbon was oxidised by 5 M nitric acid (HNO_3) at its boiling point, for 3 h; the carbon was thus termed 3HNO. The oxidized AC was doped with Fe^{3+} by forced hydrolysis of $FeCl_3$ solution.

2.3. Iron-doping of activated carbons by forced hydrolysis

Four iron-doped ACs were prepared. For each one, 5 g of oxidized carbon were introduced into 150 mL of a 0.05 M $FeCl_3$ solution in acidic media (3 M HCl) for 2 h. Forced hydrolysis was next carried out at 100 °C for different times: 1, 3, 6 and 24 h. The samples were washed to reach neutral pH and then dried at 80 °C overnight.

2.4. Characterization of the doped activated carbons

2.4.1. Elemental analysis

Elemental analysis was carried out at the "Service Central d'Analyse du CNRS" (Vernaison, France). Elemental analyzers were used for C, H and O: oxygen content was determined by quantification of carbon monoxide after it reacted with carbon at 1120 °C, and C and H levels were measured as CO_2 and H_2O gases, respectively, after their reaction with oxygen at 1050 °C. Iron, silicon, sodium and potassium were determined by ICP–AES after acid digestion.

2.4.2. Surface area and porosity

The pore texture parameters were determined from the corresponding nitrogen adsorption–desorption isotherms obtained at 77 K with an automatic instrument (ASAP 2020, Micromeritics). The samples were previously outgassed at 423 K for 24 h. Such a low degasification temperature was chosen in order to prevent changes of nanoparticle diameter. The surface areas were measured by the Brunauer–Emmet–Teller (BET) calculation method [28] applied to the adsorption branch of the isotherms. The micropore volume, V_{DR}, corresponding to pores narrower than 2 nm, was calculated according to the Dubinin–Radushkevitch (DR) method ([29] and refs. therein). The total pore volume, sometimes referred to as the so-called Gurvitch volume $V_{0.99}$, was defined as the volume of liquid nitrogen corresponding to the amount adsorbed at a relative pressure $p/p_0 = 0.99$ [30]; the Gurvitch volume is assumed to be the

Table 1
Physico-chemical parameters of a well water of Chihuahua. NS, UC, TDS and TSS mean: Not specified, Units of colours, total dissolved solids, and total suspended solids, respectively.

Parameter		Limits	Method	Reference
pH	8.03	6.5–8.5	Electrometric	NMX-AA-008-SCFI-2000
Alkalinity ($mg\,L^{-1}$ $CaCO_3$)	142	NS	Potentiometric	NMX-AA-007-SCFI-2000
Chlorides ($mg\,L^{-1}$ Cl)	21.8	250	Argentometric	NMX-AA-073-SCFI-2001
Color (UC)	<5	20	Colorimetric	NMX-AA-045-SCFI-2001
Conductivity ($\mu S\,cm^{-1}$)	427	NS	Electrometric	NMX-AA-093-SCFI-2001
Total hardness ($mg\,L^{-1}$ $CaCO_3$)	49.5	500	Volumetric	NMX-AA-072-SCFI-2001
Ca hardness ($mg\,L^{-1}$)	38.6	NS	Volumetric	SM-3500 CA b 1998
TDS ($mg\,L^{-1}$)	390	1000	Gravimetric	SM-2540 C-1998
TSS ($mg\,L^{-1}$)	0	NS	Gravimetric	NMX-AA-034-SCFI-2001
As ($\mu g\,L^{-1}$)	311.5	NS	Absorption	NOM-127-SSA1-1994

Table 2
Elemental analyses (wt.%) of the commercial, oxidised and iron-doped activated carbons.

Sample	Precursor	C	H	O	Si	K	Na	Fe
NC-100	–	93	0.60	3.2	0.10	1.47	0.10	200 ppm
3HNO	NC-100	85	0.95	9.9	0.14	<20 ppm	<200 ppm	840 ppm
Fe-1H	3HNO	89	<0.30	8.5	n.d.	n.d.	n.d.	1.5
Fe-3H	3HNO	88	<0.30	8.3	n.d.	n.d.	n.d.	2.0
Fe-6H	3HNO	87	<0.30	8.7	n.d.	n.d.	n.d.	2.2
Fe-24H	3HNO	76	0.86	10.0	n.d.	n.d.	n.d.	9.4

sum of micro plus mesopore volumes. The mesopore volume, V_{meso}, was calculated as the difference between $V_{0.99}$ and V_{DR}.

2.4.3. Transmission electron microscopy (TEM)

TEM studies were performed using a Philips CM20 transmission microscope operating at 200 kV. Semi-quantitative elemental analysis and element mapping were carried out by energy dispersive X-ray spectrometry (EDX). Samples were prepared by dispersion and sonication of AC grains in THF. A drop of the resultant suspensions was deposited on a carbon observation grid and then introduced into the microscope column.

2.4.4. X-ray diffraction (XRD) analysis

XRD patterns were obtained using a Brüker AXS D8 Advance diffractometer system using Cu K_α ray (λ = 1.5418 Å).

2.5. Arsenic removal from contaminated water with ACs.

Batch sorption experiments were performed in order to obtain kinetics and equilibrium data. 250 mL of contaminated water sample from a Chihuahuan well were introduced in 500 mL Erlenmeyer flasks kept at room temperature and magnetically stirred. AC was weighed (2 g) and added to the solution. Each flask was removed after the required reaction time (never higher than 2 h, as evidenced by the following kinetic studies), and the solution was filtered through Whatman No. 2 filter paper. Each experiment was run in duplicate, and average values were reported. All experiments were carried out at constant temperature of 25 ± 0.1 °C. Such a temperature is a bit higher than that of groundwater when collected (typically 19.5 °C), but matches room temperature, at which a commercial process using iron-doped activated carbons could work.

The amount of arsenic remaining in the solution was determined using an atomic absorption spectrometer with a hydride generator PerkinElmer 800 Analyst. The device was settled according to the following parameters: wavelength 193.7 nm; slit 0.7, argon flow 50 mL min^{-1}; pump velocity 120 rpm. For intercalibration, a standard provided by CENAM (National Metrology Centre) CNM-MR-620-0030-DMR8i with an arsenic concentration of 0.2278 ± 0.008 ppm was used. Five arsenic standards were made in the range of 0–50 ppb in a solution of 10% KI and 10% HCl (both from Sigma, AAS grade). Reaction was carried out for 45 min. Time was cautiously controlled due to time dependence of the signal [31].

3. Results and discussion

3.1. Characterisation of iron-doped activated carbon

Table 2 shows the elemental analysis (wt.%) of the commercial AC (NC-100), the oxidized (3HNO) and the iron-doped ACs prepared by forced hydrolysis. Raw NC-100 has oxygen and carbon contents of 3.2 and 93 wt.%, respectively. Si, K, Na and Fe were found to be present at low levels. Oxidation produced the elimination of almost all ashes, except silica which relative amount increased. After oxidation, the oxygen content was increased up to 9.9%. Iron content in the activated carbon increased almost linearly with increasing hydrolysis time: 1.5%, 2.0%, 2.2% and 9.4% for 1, 3, 6 and 24 h, respectively.

Table 3
Textural parameters of commercial, oxidised and doped activated ACs.

Sample	S_{BET} ($m^2 g^{-1}$)	$V_{0.99}$ ($cm^3 g^{-1}$)	V_{DR} ($cm^3 g^{-1}$)	$V_{DR}/V_{0.99}$	V_{meso} ($cm^3 g^{-1}$)
NC-100	2100	0.92	0.80	0.87	0.12
3HNO	1648	0.74	0.61	0.82	0.21
Fe-1H	1585	0.75	0.57	0.76	0.18
Fe-3H	1636	0.76	0.58	0.76	0.18
Fe-6H	1575	0.76	0.57	0.74	0.20
Fe-24H	1643	0.80	0.59	0.73	0.21

Table 3 shows the textural parameters derived from the adsorption isotherms of nitrogen at 77 K for all the ACs. Raw NC-100 has a surface area of 2100 m^2/g and it is essentially microporous. Oxidation produced a material (3HNO) having a lower surface area (1648 m^2/g); the micropore volume indeed decreased from 0.80 to 0.61 cm^3/g, whereas the mesopore volume increased from 0.12 to 0.21 cm^3/g. In spite of the high percentages of iron deposited, the forced hydrolysis of ferric chloride did not significantly change the textural parameters of the resultant ACs, since differences in surface area lower than 5% were observed, i.e., within the experimental error range of the automatic adsorption apparatus.

Fig. 1 shows the XRD patterns of the iron-doped ACs after iron (III) chloride hydrolysis was forced during 1, 3, 6 or 24 h. No difference can be observed between the ACs, suggesting either that deposited iron phase was amorphous or that the particles were really too small to diffract. In order to go deeper into the characterization of these nanoparticles, TEM observations were carried out.

Fig. 2 shows a TEM picture of Fe-3 h activated carbon sample, in which darker particles can be observed at the surface of the grain. These particles are well-distributed, iron-based, and have a nanometric size, as already suggested by XRD patterns. Fig. 3 shows TEM pictures of a sample of Fe-6 h. Fig. 3a again shows well-distributed iron-based nanoparticles together with clusters based on nanoparticles, in agreement with both XRD and nitrogen adsorption. Regardless of the size of the particles (i.e.,

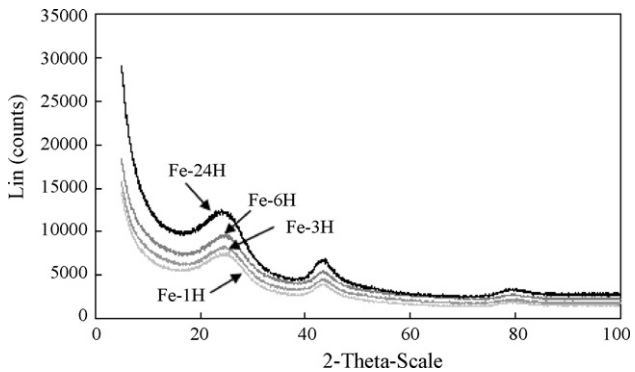

Fig. 1. XRD patterns of and iron-loaded activated carbons, after iron (III) chloride hydrolysis was forced during 1, 3, 6 and 24 h.

Fig. 2. TEM image of Fe-3 h AC.

whether nanoparticles are clustered or not), iron is seen to be very well-dispersed all throughout the carbonaceous material (Fig. 3c). Comparison with oxygen mapping (Fig. 3d) suggests that iron is closely associated with oxygen. Obviously, carbon being the support material, the corresponding mapping evidences a very homogeneous dispersion (Fig. 3b).

After 24 h of hydrolysis, big clusters having sizes ranging from 50 to 100 nm may be observed at the outer surface of the AC grain, as seen in Fig. 4a and b. Fig. 4c shows an electron microdiffraction pattern of one of these iron-based clusters of nanoparticles. The latter are seen to be well-crystallized with an hexagonal-type structure, as expected for the most usual iron oxide: α-Fe_2O_3, or for ferrihydrite: $Fe_5(OH)O_7{\cdot}4H_2O$ or goethite FeO(OH). These three compounds present closely related structures, however, given the way iron was precipitated (forced hydrolysis in mild conditions), the two latter phases are much more likely than pure, dry, iron oxide. The absence of diffraction peaks evidenced in Fig. 1 can now be attributed to the very small size of the nanoparticles. This finding further confirms that the big particles seen in Figs. 3–5 are only clusters of such extremely small iron (hydr)oxide grains. This is particularly obvious from Fig. 4(a). Fig. 5 shows another TEM picture for Fe-24 h, and its corresponding element mapping as revealed by EDX. Fig. 5a shows evenly distributed nanoparticles and bigger agglomerates; Fig. 5c and d further confirm that iron is associated with oxygen, since a frank correlation is evidenced between the locations of iron and oxygen clusters. Moreover, we already showed [22] that carbon oxidation, through the introduction of oxygen functional groups, increased iron adsorption, provided that the pHz of the AC is suitable. Other authors also showed the interaction of oxygenated functional groups with Fe [20], further supporting the iron–oxygen association.

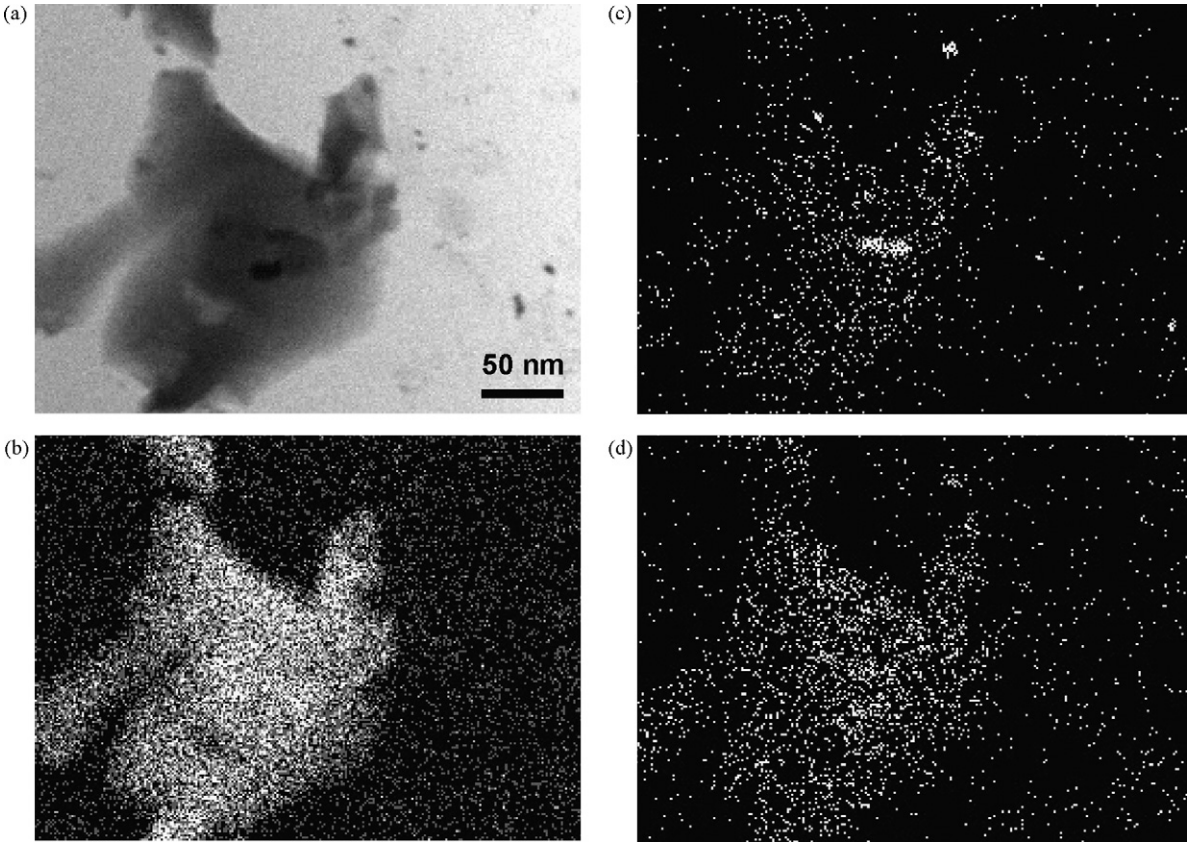

Fig. 3. TEM images of Fe-6 h AC. (a) Bright field image, and mapping of elements: (b) C, (c) O and (d) Fe, as seen by EDX (energy dispersion of X-rays).

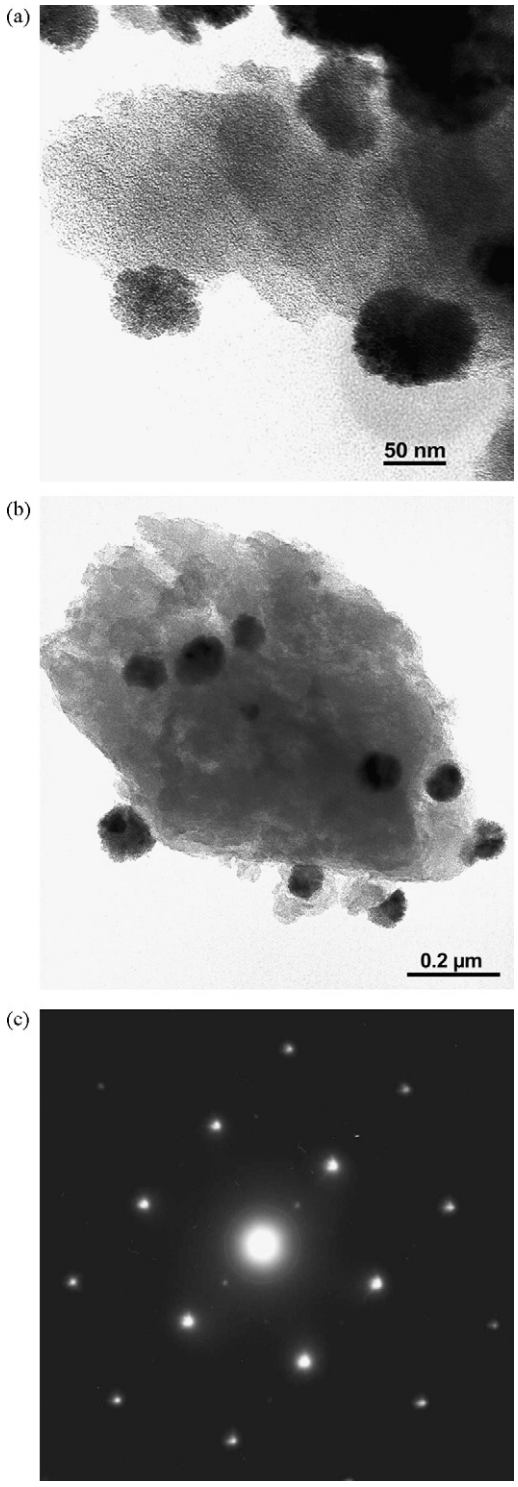

Fig. 4. TEM images of Fe-24 h AC. (a) and (b) Bright field images at different magnifications, (c) electron microdiffraction pattern of one nanoparticle.

From the characterization of the iron-doped activated carbons, it may be concluded that ferric chloride forced hydrolysis allowed increasing iron content up to 9.4 wt.% without any modification of the textural properties of the activated carbons, as determined by nitrogen adsorption at 77 K. Iron is associated to oxygen and deposited on the entire surface of the AC in the form of well-dispersed nanoparticles when hydrolysis time is lower than 6 h. At higher hydrolysis times, agglomerates of nanoparticles appeared at the outer surface of the AC grains. The nanoparticle nature of the iron (hydr)oxide allowed nitrogen diffusion and adsorption over the whole surface of the AC grains and, consequently, the measured textural parameters remained essentially unchanged. However, the behaviour in liquid phase during arsenic adsorption is very different, as it will be evidenced in next section.

3.2. Arsenic adsorption

Since dissolved arsenite (As (III)) and arsenate (As (V)) compounds have been found to be simultaneously present in many contaminated groundwaters [32], it is likely that both are indeed present in the natural well water investigated here. Given that its pH is close to 8, the predominant dissolved species should be $HAsO_2$ and $HAsO_4^{2-}$. Activated carbon was already shown to catalyse the oxidation of As (III) into As (V), even in quasi-anaerobic conditions [33]. The presence of iron (III) species, which are able to oxidise As (III), was also found to accelerate such an oxidation to As (V) [34]. Therefore, the arsenic species which finally adsorb at the surface of the present carbonaceous materials can be considered to be arsenate in the form of $HAsO_4^{2-}$ only.

Fig. 6 shows arsenic removal by iron-doped ACs as a function of time. Arsenic uptake increased when the length of forced hydrolysis was increased from 1 to 6 h. The plateau of maximal adsorption is reached after 40 min for ACs prepared at 1 and 3 h hydrolysis time. The material Fe-6H required a slightly longer time to achieve higher arsenic uptake than that of Fe-3H, suggesting a more difficult diffusion of arsenate ($HAsO_4^{2-}$) throughout the porosity of the heavier-doped AC.

As shown above, the textural parameters of doped activated ACs were essentially the same as that of their precursor, 3HNO. However, extremely different values of arsenic removal were determined here, probably due to the fact that arsenic removal takes place in the liquid, aqueous, phase. Hydration of iron (hydr)oxide nanoparticles and their clusters could make them swell, through the formation of a water-rich gel, leading to a decreased diffusion and accessibility of arsenate ($HAsO_4^{2-}$) to the pores.

The pseudo second-order equation was successfully applied to the experimental adsorption data. The pseudo second-order is represented by the following equation:

$$\frac{t}{q_t} = \frac{1}{k\,q_e^2} + \frac{t}{q_e} = \frac{1}{h} + \frac{t}{q_e} \quad (1)$$

where q_t and q_e are the adsorbed amounts at time t and at equilibrium, respectively, and k is the kinetic constant. The parameters h, q_e and k can be experimentally determined from the slope and intercept of a plot of t/q_t versus t.

Table 4 shows the kinetic parameters and the correlation coefficient (R^2) derived from application of the pseudo second-order equation to the adsorption data of all the Fe-doped ACs, the commercial AC and the oxidized AC. Excellent fits were obtained for all the ACs studied, with correlation coefficients ranging from 0.99 to 1.00. The highest initial sorption, h, was found for Fe-3H (3.81×10^{-2} mg As/g AC/min), but the maximum equilibrium sorption capacity was found for Fe-6H (0.028 mg As/g AC). An arsenic removal of only 0.008 mg As/g C was obtained with Fe-24H, although having the highest Fe content. The lowest initial sorption capacity (6.45×110^{-4} mg As/g AC/min) was also obtained for Fe-24H.

The adsorbed amounts at equilibrium are typically 1000 times lower than those reported by Pattanayak et al. [35], but such a result does not mean that the activated carbons investigated here are poor adsorbents. In fact, like most authors, e.g. Lorenzen et al. [36] amongst others, Pattanayak et al. worked with arsenic concentrations at least 1000 times higher than ours. Thus, our results compare well with those of Gu et al. [37], who used initial arsenic concentrations of 105 and 1031 ppb. Moreover, because most of

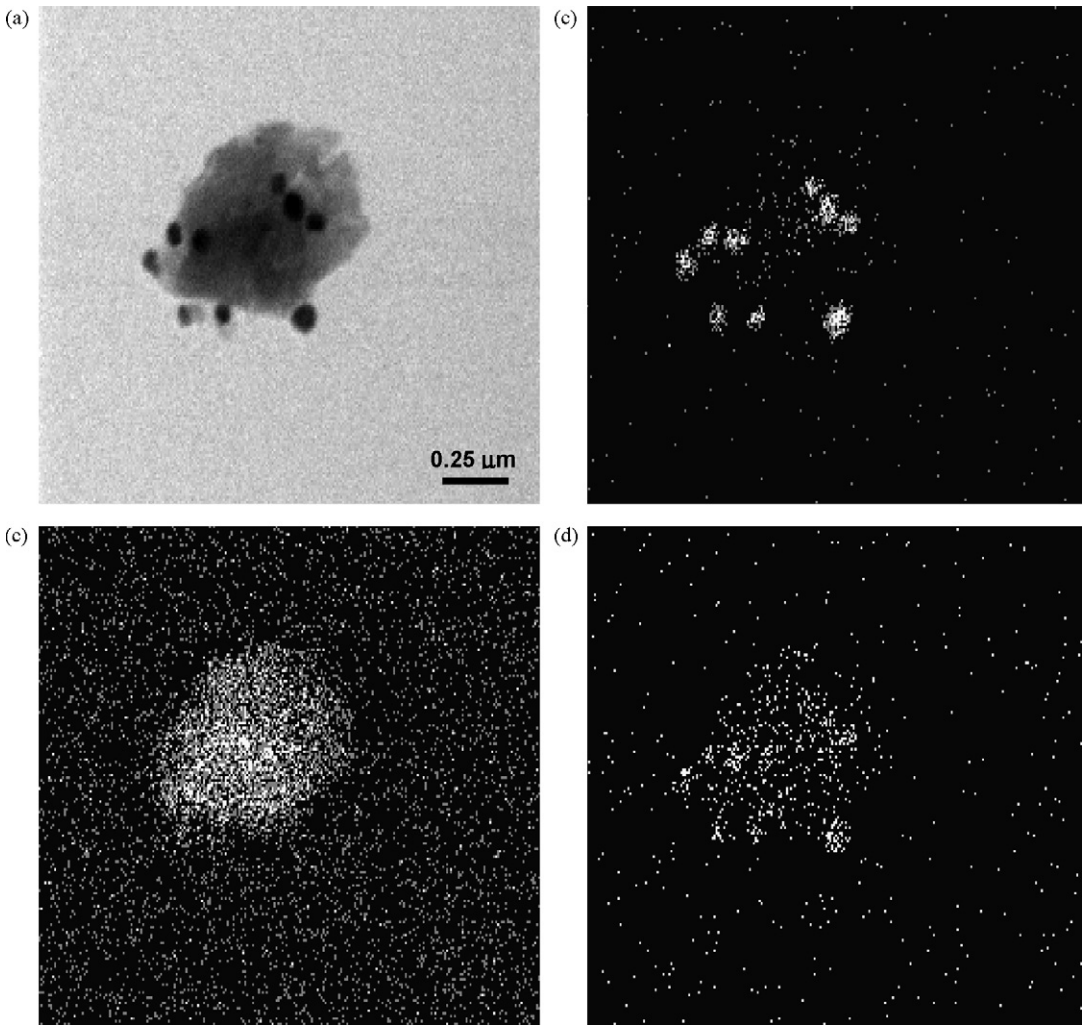

Fig. 5. TEM images of a grain of Fe-24 h AC (a) Bright field image, and mapping of elements: (b) C, (c) O and (d) Fe, as seen by EDX (energy dispersion of X-rays).

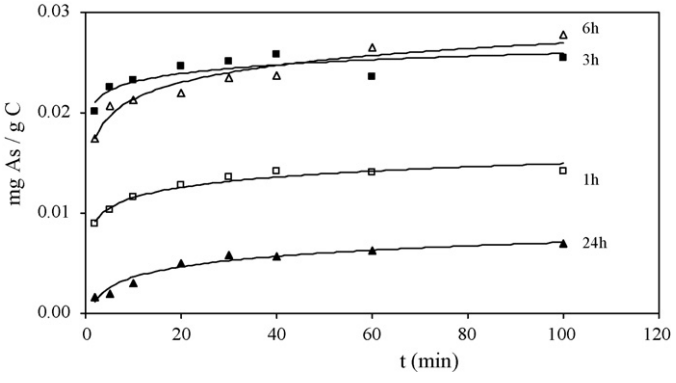

Fig. 6. As uptake, as a function of time, of the iron-doped ACs. The hydrolysis time in indicated on the plot.

Table 4
Kinetic parameters of As adsorption determined by applying the pseudo second-order.

Sample	h (mg g^{-1} min^{-1})	q_e (mg g^{-1})	k (g mg^{-1} min^{-1})	R^2
NC-100	9.86×10^{-4}	0.004	58.52	0.99
3HNO	1.08×10^{-3}	0.001	639.35	1.00
Fe-1H	7.80×10^{-3}	0.015	37.21	1.00
Fe-3H	3.81×10^{-2}	0.025	59.63	1.00
Fe-6H	7.22×10^{-3}	0.028	9.06	1.00
Fe-24H	6.45×10^{-4}	0.008	10.95	0.99

the tests reported in the literature deal with much higher initial arsenic concentrations, it is extremely difficult to compare our own results with those obtained with adsorbents traditionally used for arsenic removal. Additionally, groundwater samples used in this experiment contain other organic species whose adsorption should compete with that of arsenic oxyanions, so any comparison with other materials tested with model (lab-made) arsenic solutions is uneasy. Finally, pH higher than eight, like in the present case, was shown to be unfavourable for both As (III) and As (V) adsorption [35], thus further accounting for the apparently low arsenic uptakes reported here; the optimum pH for removal of arsenic using adsorptive media or ferric chloride as coagulant indeed ranges from 6.8 to 7.3.

Fig. 7 shows the equilibrium arsenic uptake (q_e, taken from Table 4) of iron-doped ACs as a function of their iron content, as well as that of their precursors (raw and oxidized material) for comparison. NC-100 and 3HNO adsorbed 0.004 and 0.001 mg As/g AC, respectively. The decrease of arsenic adsorption after oxidation with nitric acid was explained in terms of modification of the pH_{ZC} [22]. NC-100 had a pH_{ZC} of 10.26 and the well water used in this work had a pH of 8.03; the surface of NC-100 was thus positively charged on average, i.e., attracting anionic (mainly As (V)) species. Under these conditions, adsorption should be non specific, and hence should essentially depend on the surface area. NC-100 had a high surface area of 2100 m^2/g and a total pore volume of 0.92 cm^3/g, consequently the removal of arsenic was more effi-

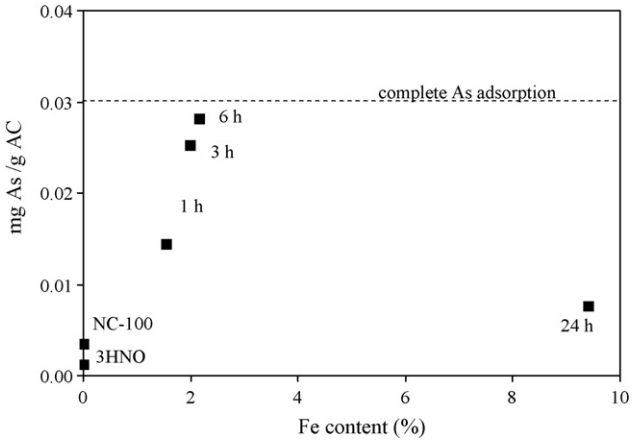

Fig. 7. Arsenic uptake of all the investigated materials (raw, oxidised, and iron-doped ACS), as a function of their Fe content.

cient than with 3HNO, which had a lower pH_{ZC} (4.33), and lower pore volume and surface area. The effect of mineral content could also play a role on the arsenic adsorption of raw AC, the higher its amount, the better the adsorption of arsenic, in agreement with a number of other results ([36,37] and refs. therein, [38]). Such an effect was thought to be due to strong interaction of arsenic species with metal oxides and ions [38], and to the net positive charge they give to the adsorbent surface at medium pH, typically from 5 to 10. The latter assertion is true only as far as basic oxides are concerned [39], e.g., alkaline or alkaline-earth oxides, having a pH_{ZC} typically higher than 10 [34]. Basic oxides were all removed after oxidation, and only silica remained in non negligible amount. Silica has a pH_{ZC} of 2.2, and thus presents a negatively charged surface, which is unfavourable for arsenate adsorption.

After 1 h of hydrolysis time, iron content increased up to 1.5%, and so did the arsenic sorption capacity: 0.015 mg/g. Arsenic removal efficiency was thus multiplied almost by four and fifteen, taking NC-100 or 3HNO as reference materials. Such an increase is attributed to a change of arsenic removal mechanism, from non specific (i.e., all over the available surface) to specific (i.e., by interaction of As with Fe). When iron (hydr)oxides are present, surface complexation of arsenic oxyanions is expected. However, as reported by Sperlich et al. [40] there is no consensus in the literature about the relevant interaction mechanisms. Thus, surface precipitation was also suspected to occur.

Increasing hydrolysis time from 1 to 3, and then to 6 h, made the iron content also increase from 1.5 to 2.0 and to 2.2%, respectively. Correspondingly, the arsenic sorption capacity increased linearly with iron content, from 0.015 to 0.025 and 0.028 mg As/g AC. When the hydrolysis time was as long as 24 h, the iron content increased up to 9.8%; however, the arsenic uptake at equilibrium was much lower than before, decreasing down to 0.008 mg As/g AC. Such a drop is probably due to the existence of large iron (hydr)oxides agglomerates of nanoparticles. These agglomerates, once hydrated, could prevent arsenate ($HAsO_4^-$) ions from diffusing towards the inner surface of the AC grains. In that way, a great part of the surface area is not available for arsenic removal, and the performances of the AC is expected to decrease.

4. Conclusions

Ferric chloride forced hydrolysis is a good method for increasing the iron content of activated carbons. Activated carbons with iron contents ranging from 1.5 to 9.4% were thus obtained; the amount of deposited iron increased linearly with hydrolysis time. Iron-based nanoparticles, homogeneous in size, extremely small and well-dispersed in the carbon matrix, were obtained. Nanoparticles forming clusters over the outer surface of the carbon grains at hydrolysis times higher than 6 h were also produced. Agglomerates with a size ranging from 50 to 100 nm and composed of iron (hydr)oxyde nanoparticles were found in the AC prepared by forced hydrolysis during 24 h.

Ferric chloride forced hydrolysis thus allowed preparing iron-doped ACs with improved performances for removing arsenic from groundwater. 14% of the arsenic present in a groundwater could be removed using the commercial activated carbon. But once the latter was oxidized and doped with iron by forced hydrolysis of ferric chloride during 6 h, the removal reached 94% of the initial arsenic concentration. Arsenic removal from natural well water was found to be a linear function of iron content, up to 2.2 wt.% of iron contained in the AC. The latter value corresponds to the AC prepared by ferric chloride forced hydrolysis during 6 h; resistance to diffusion of adsorbate was observed for this material. Higher iron contents within the AC, especially for the material obtained after 24 h of hydrolysis, led to much lower arsenic uptakes. This phenomenon is probably due to the existence of iron hydr(oxides) clusters of nanoparticles, which once hydrated could hinder and even prevent arsenate ($HAsO_4^-$) ions diffusion towards the inner surface of the AC grains.

Further studies on arsenic adsorption in a column and on leaching are yet required for studying the feasibility and applicability of these activated carbons at a commercial scale. Especially, several key points will have to be investigated in detail: cost, toxicity characteristic leaching procedure after use, rapid small scale column test in more realistic conditions of water treatment, and maximum concentration limit that should be below 10 μg/L in drinking water.

Acknowledgements

The authors gratefully acknowledge the financial support from the European Commission through the ALFA program (project LIGNOCARB-ALFA II 0412 FA FI).

References

[1] Comisión Nacional del Agua, CNA. Estudio Hidrológico, Hidrogeoquímico y de la incidencia de arsénico, flúor y hierro en las zonas acuíferas de Delicias-Meoqui y Jiménez-Camargo, Chih. Gerencia de Aguas Suterráneas, Chihuahua, México, 1996 (in Spanish).
[2] EPA-542-S-02-002 October 2002 (revised) Proven alternatives for above ground treatment of arsenic in ground water in: http://www.epa.gov/tio/tsp.
[3] B.A. Manning, S. Goldberg, Adsorption and stability of arsenic (III) at the clay mineral water interface, Environ. Sci. Technol. 31 (1997) 2005–2011.
[4] B.A. Manning, S.E. Fendorf, S. Goldberg, Surface structures and stability of arsenic (III) on goethite: spectroscopic evidence for inner-sphere complexes, Environ. Sci. Technol. 32 (1998) 2383–2388.
[5] J.A. Wilkie, J.G. Hering, Adsorption of arsenic onto hydrous ferric oxide: effects of adsorbate/adsorbent ratios and co-occurring solutes, Colloids Surf. A: Physicochem. Eng. Aspects 107 (1996) 97–110.
[6] J.A. Lackovic, N.P. Nikolaidis, G.M. Dobbs, Inorganic arsenic removal by zerovalent iron, Environ. Eng. Sci. 17 (2000) 29–39.
[7] C. Su, R.W. Puls, Arsenate and arsenite removal by zero valent iron: kinetics, redox transformation, and implications for in situ groundwater remediation, Environ. Sci. Technol. 35 (2001) 1487–1492.
[8] C. Su, R.W. Puls, Arsenate and arsenite removal by zerovalent iron: effects of phosphate, silicate, carbonate, borate, sulfate, chromate, molybdate, and nitrate, relative to chloride, Environ. Sci. Technol. 35 (2001) 2568–4562.
[9] W. Driehaus, M. Jekel, J. Hildebrandt, Granular ferric hydroxide—a new adsorbant for the removal of arsenic from natural water, J. Water Supply Res. Technol.-Aqua 47 (1998) 30–35.
[10] O.S. Thirunavukkarasu, T. Viraraghavan, K.S. Subramanian, Removal of arsenic in drinking water by iron oxide-coated sand and ferrihydrite-batch studies, Water Qual. Res. J. Can. 36 (2001) 55–70.
[11] K.P. Raven, A. Jain, R.H. Loeppert, Arsenite and arsenate adsorption on ferrihydrite: kinetics, equilibrium, and adsorption envelopes, Environ. Sci. Technol. 32 (1998) 344–349.
[12] M. Badruzzamana, P. Westerhoffa, D.R.U. Knappeb, Intraparticle diffusion and adsorption of arsenate onto granular ferric hydroxide (GFH), Water Res. 38 (2004) 4002–4012.

[13] D. Mohan, C.U. Pittman, Arsenic removal from water/wastewater using adsorbents—a critical review, J. Hazard. Mater. 142 (2007) 1–53.
[14] T.S.Y. Choong, T.G. Chuah, Y. Robiah, F.L.G. Koay, I. Azni, Arsenic toxicity, health hazards and removal techniques from water: an overview, Desalination 217 (2007) 139–166.
[15] S.K. Gupta, K.Y. Chen, Arsenic removal by adsorption, J. Water Pollut. Control Fed. 50 (1978) 493–506.
[16] J.Y. Lee, R.G. Rosehart, Arsenic removal by sorption processes from waste waters, Can. Min. Metall. Bull. 65 (1972) 33–37.
[17] C.P. Huang, P.L.K. Fu, Treatment of arsenic(V)-containing water by the activated carbon process, J. Water Pollut. Control Fed. 56 (1984) 233–242.
[18] C.P. Huang, L.M. Vane, Enhancing As^{5+} removal by a Fe^{2+}-treated activated carbon, J. Water Pollut. Control Fed. 61 (1989) 1596–1603.
[19] R.L. Vaughan, B.E. Reed, Modeling As(V) removal by an iron oxide impregnated activated carbon using the surface complexation approach, Water Res. 39 (2005) 1005–1014.
[20] Z. Gu, J. Fan, B. Deng, Preparation and evaluation of GAC-Based iron containing adsorbents for arsenic removal, Environ. Sci. Technol. 39 (2005) 3833–3843.
[21] B.E. Reed, R.L. Vaughan, L.Q. Jiang, As(III), As(V), Hg, and Pb removal by Fe-oxide impregnated activated carbon, J. Environ. Eng. ASCE 126 (2000) 869–873.
[22] G. Muñiz, V. Fierro, A. Celzard, G. Furdin,G. Gonzalez-Sánchez, M.L. Ballinas-Casarrubias, Synthesis, characterization and performance in arsenic removal of iron-doped activated carbons prepared by impregnation with Fe(III) and Fe(II), J. Hazard. Mater., in press.
[23] E. Matijević, P. Scheiner, Ferric hydrous oxide sols1, 2 III. Preparation of uniform particles by hydrolysis of Fe(III)-chloride, -nitrate, and -perchlorate solutions, J. Colloid Interface Sci. 63 (1978) 509–524.
[24] M. Ozaki, S. Kratohvil, E. Matijević, Formation of monodispersed spindle-type hematite particles, J. Coll. Interface Sci. 102 (1984) 146–151.
[25] M.A. Blesa, E. Matijevic, Phase transformations of iron oxides, oxohydroxides, and hydrous oxides in aqueous media, Adv. Colloid Interface Sci. 29 (1989) 173–221.
[26] C.M. Flynn Jr., Hydrolysis of inorganic iron(III) salts, Chem. Rev. 84 (1984) 31–41.
[27] M. Jang, W.F. Chen, F.S. Cannon, Preloading hydrous ferric oxide into granular activated carbon for arsenic removal, Environ. Sci. Technol. 42 (2008) 3369–3374.
[28] S. Brunauer, P.H. Emmet, E. Teller, Adsorption of gases in multimolecular mayers, J. Am. Chem. Soc. 60 (1938) 309–319.
[29] M.M. Dubinin, Fundamentals of the theory of adsorption in micropores of carbon adsorbents—characteristics of their adsorption properties and microporous structures, Carbon 27 (1989) 457–467.
[30] S.J. Gregg, K.S.W. Sing, Adsorption, Surface Area and Porosity, 2nd ed., Academic Press, London, 1982.
[31] K.F. Akter, X. Chen, L. Smith, D. Davey, R. Naidu, Speciation of arsenic in ground water samples: a comparative study of CE-UV, HG-AAS and LC–ICP-MS, Talanta 68 (2005) 406–415.
[32] J.G. Hering, V.Q. Chiu, Arsenic occurrence and speciation in municipal groundwater-based supply system, J. Environ. Eng. ASCE 126 (2000) 471–474.
[33] B. Daus, R. Wennrich, H. Weiss, Sorption materials for arsenic removal from water: a comparative study, Water Res. 38 (2004) 2948–2954.
[34] P. Mondal, C. Balomajumder, B. Mohanty, A laboratory study for the treatment of arsenic, iron, and manganese bearing ground water using Fe^{3+} impregnated activated carbon: effects of shaking time, pH and temperature, J. Hazard. Mater. 144 (2007) 420–426.
[35] J. Pattanayak, K. Mondal, S. Mathew, S.B. Lalvani, A parametric evaluation of the removal of As(V) and As(III) by carbon-based adsorbents, Carbon 38 (2000) 589–596.
[36] L. Lorenzen, J.S.J. van Deventer, W.M. Landi, Factors affecting the mechanism of the adsorption of arsenic on activated carbon, Miner. Eng. 8 (1995) 557–569.
[37] Z. Gu, B. Deng, J. Yang, Preparation and evaluation of GAC-based iron containing adsorbents for arsenic removal, Environ. Sci. Technol. 39 (2005) 3833–3843.
[38] E. Diamadopoulos, P. Samaras, G.P. Sakellaropoulos, The effect of activated carbon properties on the adsorption of toxic substances, Water Sci. Tech. 25 (1) (1992) 153–160.
[39] D. Kalderis, D. Koutoulakis, P. Paraskeva, E. Diamadopoulos, E. Otal, J.O. del Valle, C. Fernández-Pereira, Adsorption of polluting substances on activated carbons prepared from rice husk and sugarcane bagasse, Chem. Eng. J., doi:10.1016/j.cej.2008.01.007, in press.
[40] A. Sperlich, A. Werner, A. Genz, G. Amy, E. Worch, M. Jekel, Breakthrough behavior of granular ferric hydroxide (GFH) fixed-bed adsorption filters: modeling and experimental approaches, Water Res. 39 (2005) 1190–1198.